Fig. S1. Replication-activated transgene expression using inverted repeats (IR).
A. In the parental Ad.IR vector the transgene is inserted in the opposite (3'→5') direction causing termination of transgene transcription at the polyadenylation (pA) signal.
B. During viral DNA replication in cancer cells, homologous recombination between the two inverted repeats (IR) mediates the formation of a rearranged viral genome.
C. In the recombination product, the transgene is in the correct (5'→3') orientation relative to the strong RSV promoter, allowing expression of the transgene.

Fig. S1

Vector	Genomic organization	Function
A Replication-deficient, transgene-devoid Ad vector (E1/E3-deleted)		**Control vector**
Ad.zero	ΔE1 RSV pA ITR — ΔE3 ITR	The adenoviral protein capsid and the genome of Ad5.zero is identical to all other vectors except for the absence of an inserted transgene.
B Replication-deficient, reporter gene expressing Ad vectors (E1/E3-deleted)		**Expression of reporter protein**
Ad.GFP	ΔE1 CMV 5'→3' GFP pA ΔE3	Reporting cell transduction with vector via replication-independent expression of green fluorescent protein.
Ad.lacZ	RSV 5'→3' lacZ pA	Reporting cell transduction with vector via replication-independent expression of E.coli lacZ enzyme.
Ad.IR-GFP	RSV IR pA GFP 3'→5' IR	Reporting genomic vector-replication via IR-dependent GFP expression (see Fig. S1).
Ad.IR-lacZ	RSV IR pA lacZ 3'→5' IR	Reporting genomic vector-replication via IR-dependent lacZ expression (see Fig. S1).
C Replication-deficient, adjuvant expressing Ad vectors (E1/E3-deleted)		**Expression of adjuvant**
Ad.αCD3	ΔE1 RSV 5'→3' αCD3 pA ΔE3	Replication-independent expression of membrane-bound αCD3scFv (see Fig. S3).
Ad.αCD137	RSV 5'→3' αCD137 pA	Replication-independent expression of membrane-bound αCD137scFv (see Fig. S3).
Ad.IL-15	RSV 5'→3' IL-15 pA	Replication-independent expression of secreted mouse IL-15 protein.
Ad.Light	RSV 5'→3' Light pA	Replication-independent expression of secreted Light protein.
D Replication-competent, oncolytic Ad-vectors (E1A expressing)		**Replication in tumor cells**
Ad.IR-E1A/AP	ΔE1 RSV IR pA E1A IRES AP 3'→5' IR ΔE3	Viral replication and E1A/AP expression specifically in cancer cells due to IR-recombination (Fig. S1)
Ad.IR-E1A/TRAIL	RSV IR pA E1A IRES TRAIL 3'→5' IR	Viral replication and E1A/TRAIL expression specifically in cancer cells due to IR-recombination (Fig. S1)
H101	ΔE1 (partial) — ΔE3 (partial)	Viral replication specifically in cancer cells due to E1/E3 mutations

Fig. S2. Genomic structure and function of human Ad serotype 5-based vectors.
Abbreviations: AP, human placental alkaline phosphatase; *E1A*, human adenovirus serotype 5 (Ad5) early region 1A; *CMV*, cytomegalie virus promoter; *GFP*, green fluorescent protein; *IL-15*, mouse interleukin 15; *IR*, inverted repeats; *IRES*, internal ribosome entry site; *ITR*, left and right end adenoviral inverted terminal repeats; *lacZ*, E.coli beta-D-galactosidase; *LIGHT*, mouse tumor necrosis factor (ligand) superfamily member 14 (TNFSF14); *TRAIL*, human tumor necrosis factor ligand superfamily member 10 (TNFSF10); *pA*, bidirectional SV40 polyadenylation signal; *RSV*, Rous sarcoma virus long terminal repeat promoter; *αCD137scFv*, membrane-bound anti-mouse CD137(4-1BB)scFv fusion protein (Fig. S3); *αCD3scFv*, membrane-bound anti-mouse CD3scFv fusion protein (Fig. S3); *ΔE1*, E1A/E1B deletion; *ΔE3*, E3 deletion.
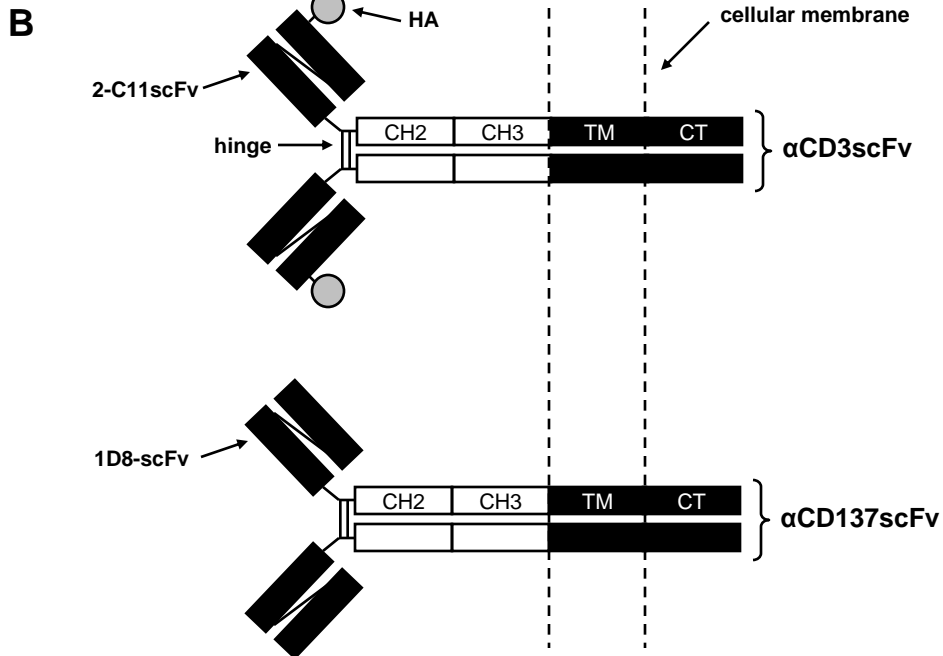
Fig. S2

Fig. S3. Illustration of membrane-bound antibody constructs.
A. Anti-CD3scFv and Anti-CD137scFv cDNA: These constructs encode for a scFv against mouse CD3 (hybridoma 2-C11) or CD137 (hybridoma 1D8), the hinge and CH2 and CH3 domains of the human IgG1 heavy chain (IgG Fc), and the murine B7-1 (CD80) transmembrane (TM) domain and cytoplasmic tail (CT). The anti-CD3scFv construct also contains a murine immunoglobulin κ chain signal peptide (SP) and a 9 amino acid HA epitope (HA).
B. Corresponding anti-CD3scFv and anti-CD137scFv fusion proteins. Anti-CD3scFv and anti-CD137scFv form disulfide-linked dimers on the cell surface.
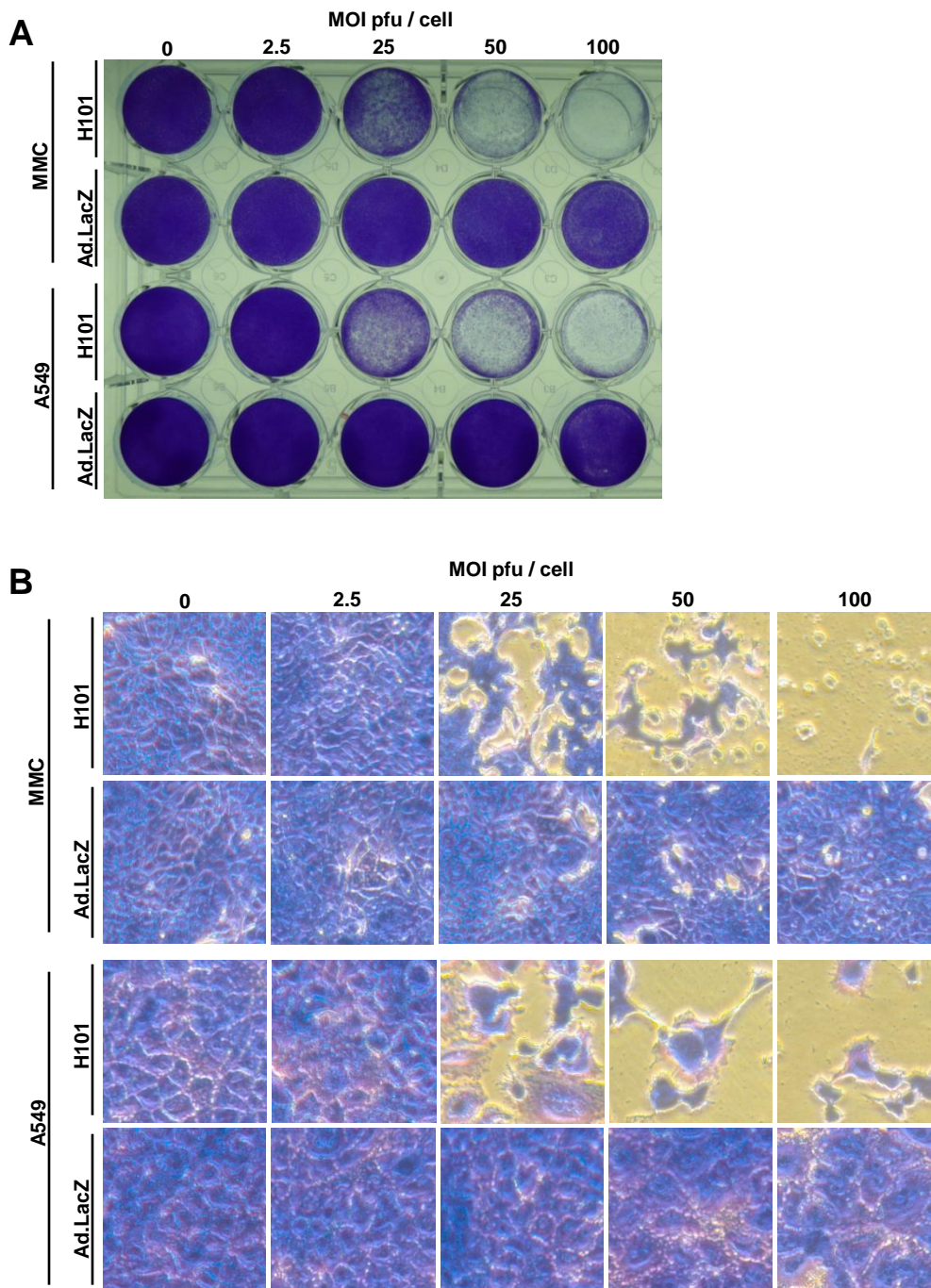
Fig. S3

Fig. S4. CPE assay.
Mouse MMC and human A549 cells were seeded in 24 well plates and infected with Ad.lacZ or H101 at indicated MOIs. Cells were fixed and stained with crystalviolet staining solution 3 days post infection. *A.* Pictures of wells. *B.* Magnification (20x) of wells. Representative pictures are shown.

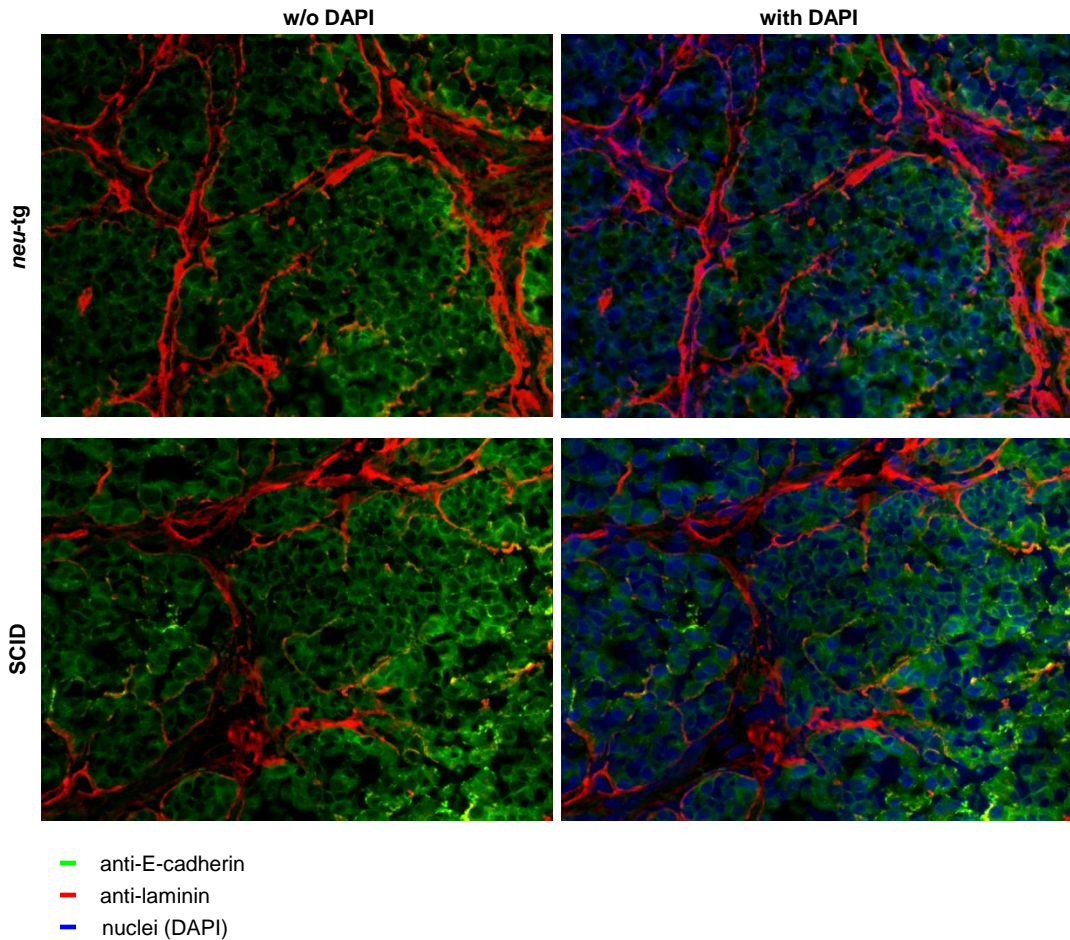**Fig. S4**

w/o DAPI **with DAPI**

neu-tg

SCID

   — anti-E-cadherin
   — anti-laminin
   — nuclei (DAPI)

Fig. S5. Detection of E-cadherin and laminin in MMC tumors using immunohistofluorescence.
MMC tumors were established in *neu*-tg mice (*upper panel*) and SCID mice (*lower panel*) and harvested two weeks later. Tumors were cryofixed, sectioned and stained for E-cadherin (green), laminin (red), and nuclei (blue). Note that MMC cells were epithelial (as indicated by bright E-cadherin surface staining) and formed clusters (nodules) surrounded by extracellular matrix (as indicated by laminin staining) in both *neu*-tg and SCID mice *in vivo*. Corresponding isotype controls yielded no significant staining. *N*=2 animals per group. Representative pictures are shown. Magnification 20x.
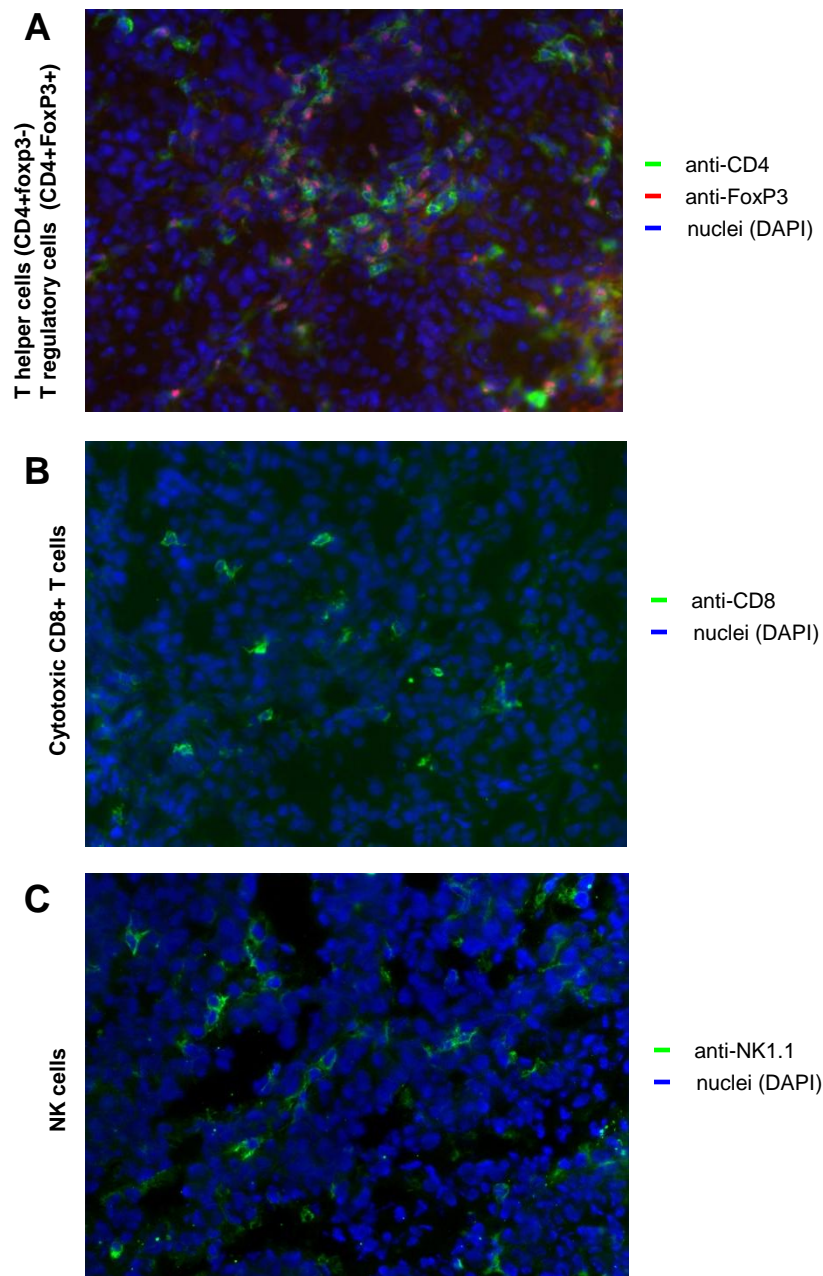
Fig. S5

Fig. S6. CD4⁺FoxP3⁻/⁺, CD8⁺ T cell and NK cell infiltration into the microenvironment of MMC tumors.
Neu-tg mice were s.c. injected with 5×10^5 MMC cells. Tumors were harvested 14 days later, cryofixed, sectioned and stained. The following directly conjugated antibodies were used: anti-CD4-FITC (clone RM4-5), anti-CD8-FITC (clone 53-6.7), anti-NK1.1-FITC (clone PK136) (all from BD Biosciences). For FoxP3 staining rabbit anti-mouse FoxP3 (provided by Dr. Kouji Matsushima, University of Tokyo) was used as a primary antibody and goat anti-rabbit-IgG AlexaFluor568 antibody (1:200; Molecular Probes, Carlsbad, CA) as a secondary antibody. Corresponding isotype controls yielded no significant staining. *N*=2 animals per group. Representative pictures are shown. 40x magnifications. *A.* CD4⁺Foxp3⁻ and CD4⁺FoxP3⁺ T cells (Note that red anti-FoxP3 staining is localized in the nuclei of approx. 50% of CD4⁺ T cells). *B.* CD8⁺ T cells (green anti-CD8 surface staining). *C.* NK cells (green anti-NK1.1 surface staining). Note that all lymphocyte populations directly co-localized with MMC tumor cells, indicating infiltration into the tumor microenvironment.
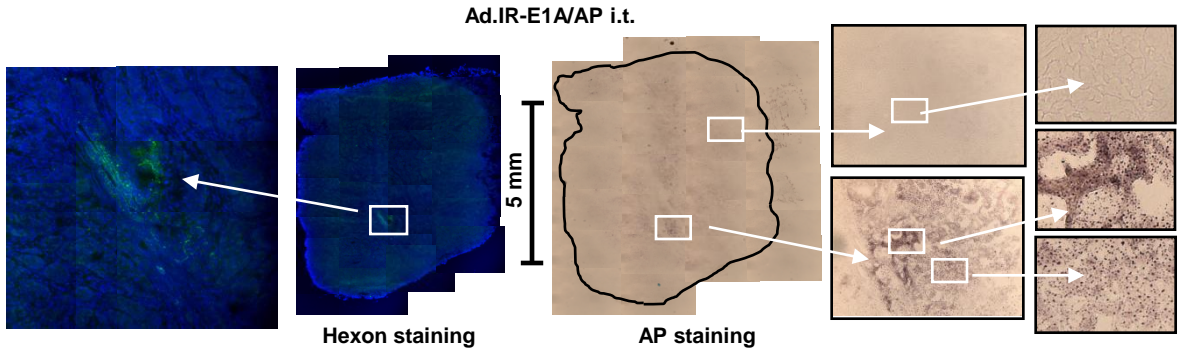
Fig. S6

Ad.IR-E1A/AP i.t.

Hexon staining

AP staining

5 mm

Fig. S7. Detection of Hexon and AP expression in Ad.IR-E1A/AP injected MMC tumors.
MMC tumors were established in *ne*u-tg mice and injected once with 1x10^9 pfu of Ad.IR-E1A/AP once when tumors reached a size of 3-4 mm diameter. Tumors were harvested 3 days later, cryofixed, sectioned and stained for Hexon and AP expression: Hexon (green), AP staining (brown), Nuclei (blue). Corresponding sections show that hexon and AP staining co-localized inside the tumor. *N*=2 animals. Representative whole tumor sections (*middle panel)* and 20x/40x magnifications *(side panels)* are shown.
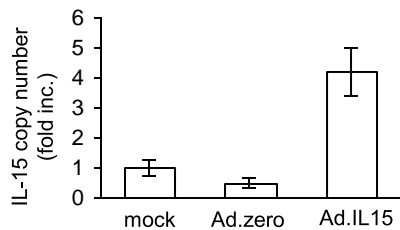
Fig. S7

Fig. S8. Quantification of intratumoral IL-15 expression via real-time RT PCR.
MMC tumors were established in *ne*u-tg mice. 1×10^9 pfu of Ad.zero or Ad.IL-15 or mock was intratumorally injected once when tumors reached a size of 3-4 mm diameter (*n*=2 animals per group). Tumors were harvested 2 days later, RNA extracted and IL-15 transcripts were relatively quantified using real-time RT PCR. y=1 for mock injected tumors. Bars indicate mean and SD.
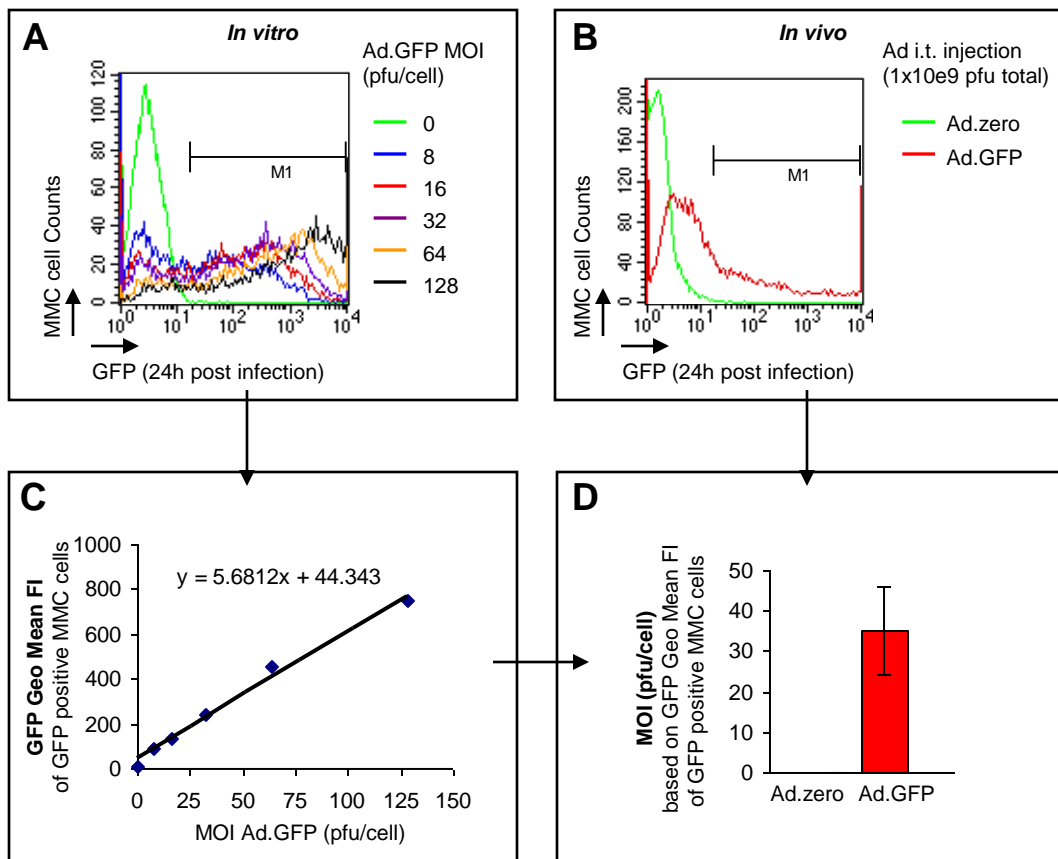
Fig. S8

Fig. S9. Quantification of MMC tumor cell transduction using Ad.GFP *in vivo*.
A. Mouse MMC cells were seeded in 24 well plates and infected 24 h later with Ad.GFP at the indicated multiplicities of infection (MOI, pfu/cell; *n*=2 per MOI). 24 h later cells were harvested and analyzed for mean GFP fluorescence intensity (FI). Overlay of representative flow charts for GFP fluorescence is shown. *B.*1x10^9 pfu Ad.GFP (*n*=3) or Ad.zero (*n*=3) was injected into MMC tumors (3-4 mm diameter) in *neu*-tg mice. 24 h later tumors were harvested, single cell suspensions generated and mean GFP FI of (E-cadherin positive) MMC cells determined. Overlay of representative flow charts for GFP fluorescence is shown. *C.* Standard curve of mean GFP FI versus Ad.GFP MOI was generated using infected MMC cells. Blue dots indicate mean values (SD was less than 5% in all cases). *D.* Mean Ad.GFP MOI of *in vivo* infected MMC tumor based was calculated based on mean GFP FI and standard curve. The result showed that MMC cells were transduced with a mean MOI of 35.3±11 pfu/cell *in vivo*. Bars indicate mean and SD.
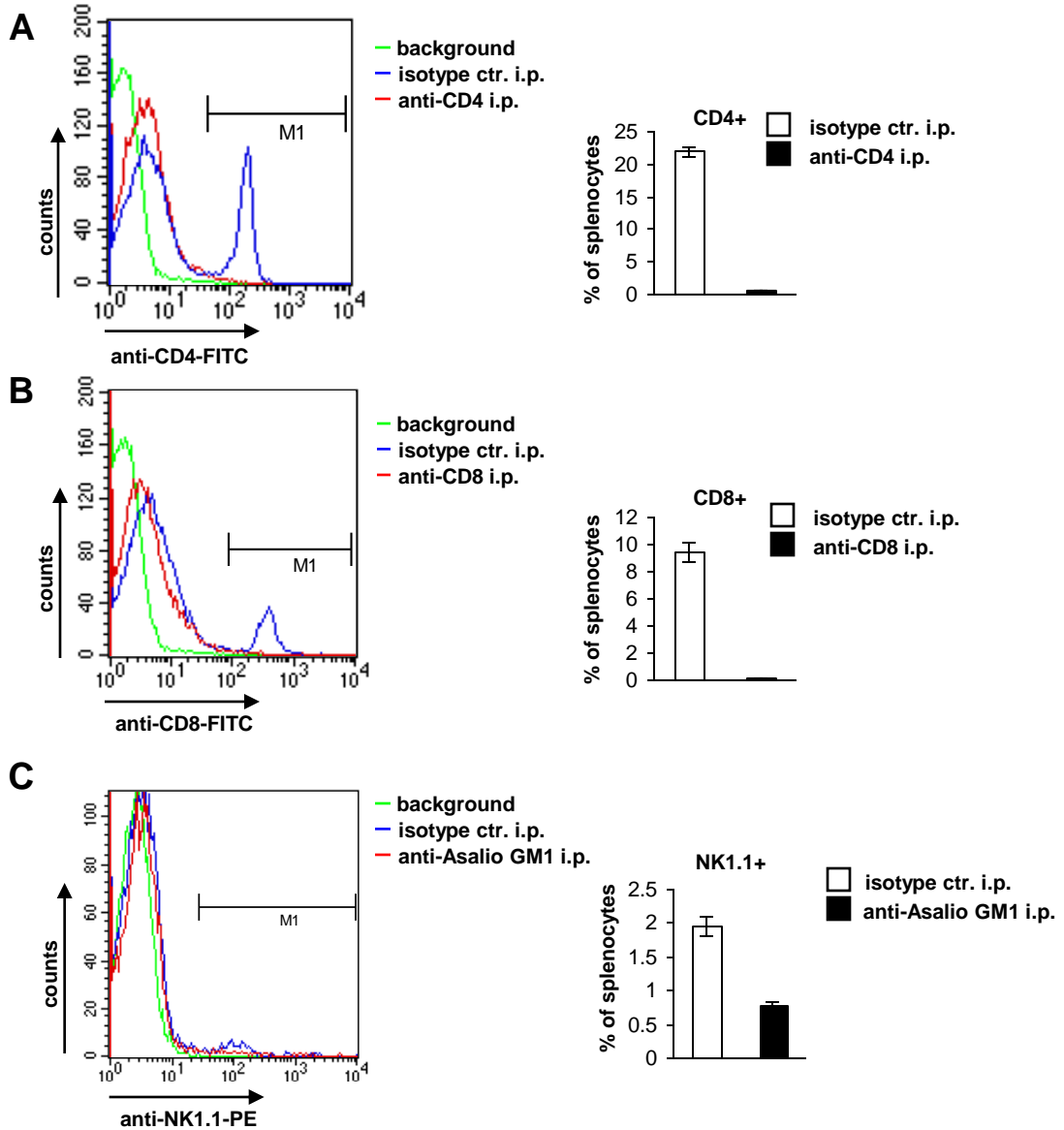
Fig. S9

Fig. S10. Depletion of CD4+, CD8+ T cells and NK cells in *neu*-transgenic mice.
A. CD4+ T cell depletion; *B.* CD8+ T cell depletion; *C.* NK cell depletion. *A-C.*
Neu-transgenic mice were injected i.p. once with 200 µg anti-mouse CD4 IgG, 200 µg anti-mouse CD8 IgG or 20 µl rabbit anti-mouse asalio GM1 IgG or 200 µg of the respective IgG isotype control. Splenocytes were extracted 4 days later and analyzed for the percentage of CD4+ T cells, CD8+ T cells and NK cells. *N*=2 animals per group. *Left panels:* Overlays of representative flow charts are shown; *Right panels:* Bars indicate mean percentage and SD. Note that for depletion and detection of CD4+ and CD8+ T cells and NK cells different hybridoma clones were utilized, respectively: *Detection:* CD4+ (RM4-5), CD8+ (53-6.7), NK (PK136). *Depletion:* CD4+ (GK1.5), CD8+ (169.4), NK (anti-asalio GM1).
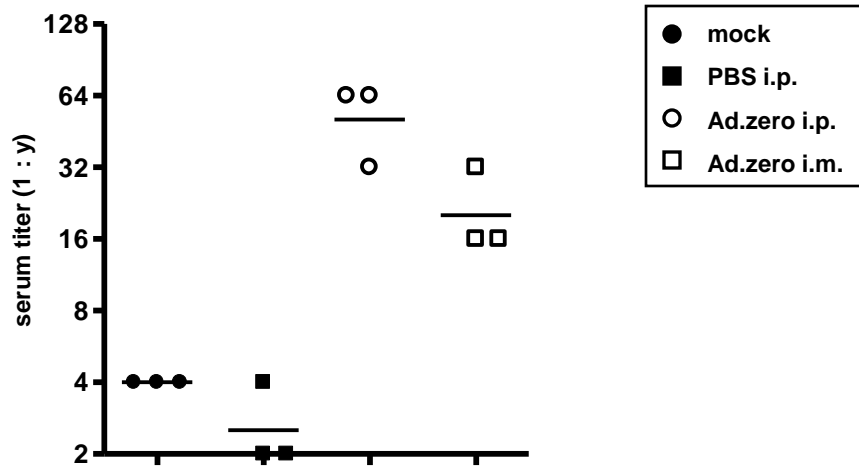
Fig. S10

Fig. S11. Ad-neutralizing antibodies in Ad-immunized and non-immunized mice.
Neu-tg mice were i.m. or i.p. injected with Ad.zero (day0 and day14). Control animals were mock or i.p. injected with PBS (day 0 and day 14). Serum was extracted from mice 14 days after the second immunization (day 28), and the titers of Ad-neutralizing antibodies were determined. *N*=3 animals per group. Lines indicate geometric means of serum dilutions that inhibited CPE formation.
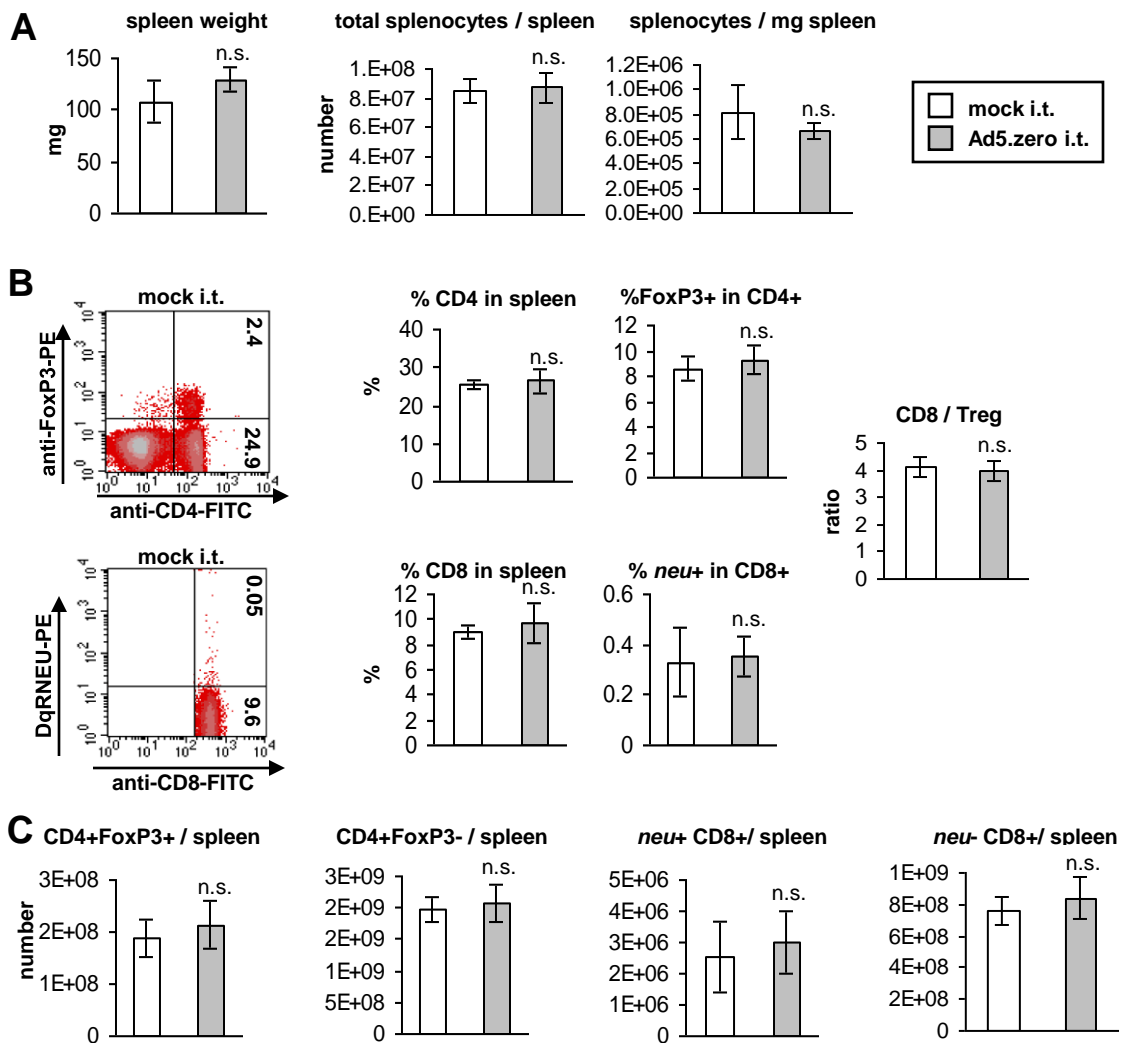
Fig. S11

A

spleen weight

total splenocytes / spleen

splenocytes / mg spleen

☐ mock i.t.
▨ Ad5.zero i.t.

B

% CD4 in spleen

%FoxP3+ in CD4+

CD8 / Treg

% CD8 in spleen

% *neu*+ in CD8+

C

CD4+FoxP3+ / spleen

CD4+FoxP3- / spleen

neu+ CD8+/ spleen

neu- CD8+/ spleen

Fig. S12. Ad-induced T cell responses in the spleen of intratumorally Ad-injected mice.
5×10^5 MMC cells were injected subcutaneous into *neu*-tg mice and 1×10^9 pfu of Ad.zero or PBS was intratumorally injected once when tumors reached a size of 3-4 mm diameter. LN (see Fig. 6) and spleens were harvested 6 days after injection (*n*=5 animals/group). **A.** Spleen weight (*left panel*), total splenocyte number per spleen (*middle panel*) and splenocytes per mg spleen (*right panel*). **B.** Percentages of *neu*/+CD8+ T cells, regulatory T cells (CD4+FoxP3+) and T helper cells (CD4+Foxp3-) were determined using flow cytometry. *Left panel.* Representative flow charts are shown. *Left panel:* Representative flow charts are shown. *Middle panel:* Mean percentages of CD4+ and CD8+ T cells in TIL, Foxp3+ in CD4+ and *neu*+ in CD8+ T cells are indicated. *Right panel:* Ratio of CD8 / Treg was calculated. **C.** Total amount of different splenocyte populations per spleen was calculated using the data from *A* and *B*. *A-C.* Bars indicate mean values and SD. *P*>0.05, *n.s.* (not significant); *, *P*<0.05; **, *P*<0.01; ***, *P*<0.001 (two-sided Student's *t*-test).
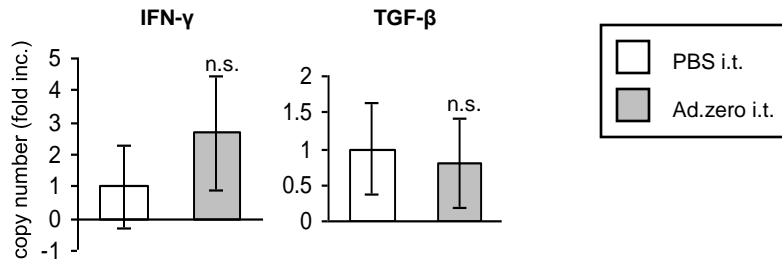
Fig. S12

Fig. S13. Quantification of intratumoral IFN-γ and TGF-β1 cytokine expression via real-time RT PCR.
MMC tumors were established in *ne*u-tg mice and 1×10^9 pfu Ad.zero or PBS was once intratumorally injected when tumors reached a size of 3-4 mm diameter (*n*=5 animals per group). Tumors were harvested 8 days later, RNA extracted and IFN-γ and TGF-β1 transcripts were relatively quantified using real-time RT PCR. y=1 for PBS injected tumors. Bars indicate mean and SD. *n.s.* (not significant; two-sided Student's *t*-test).
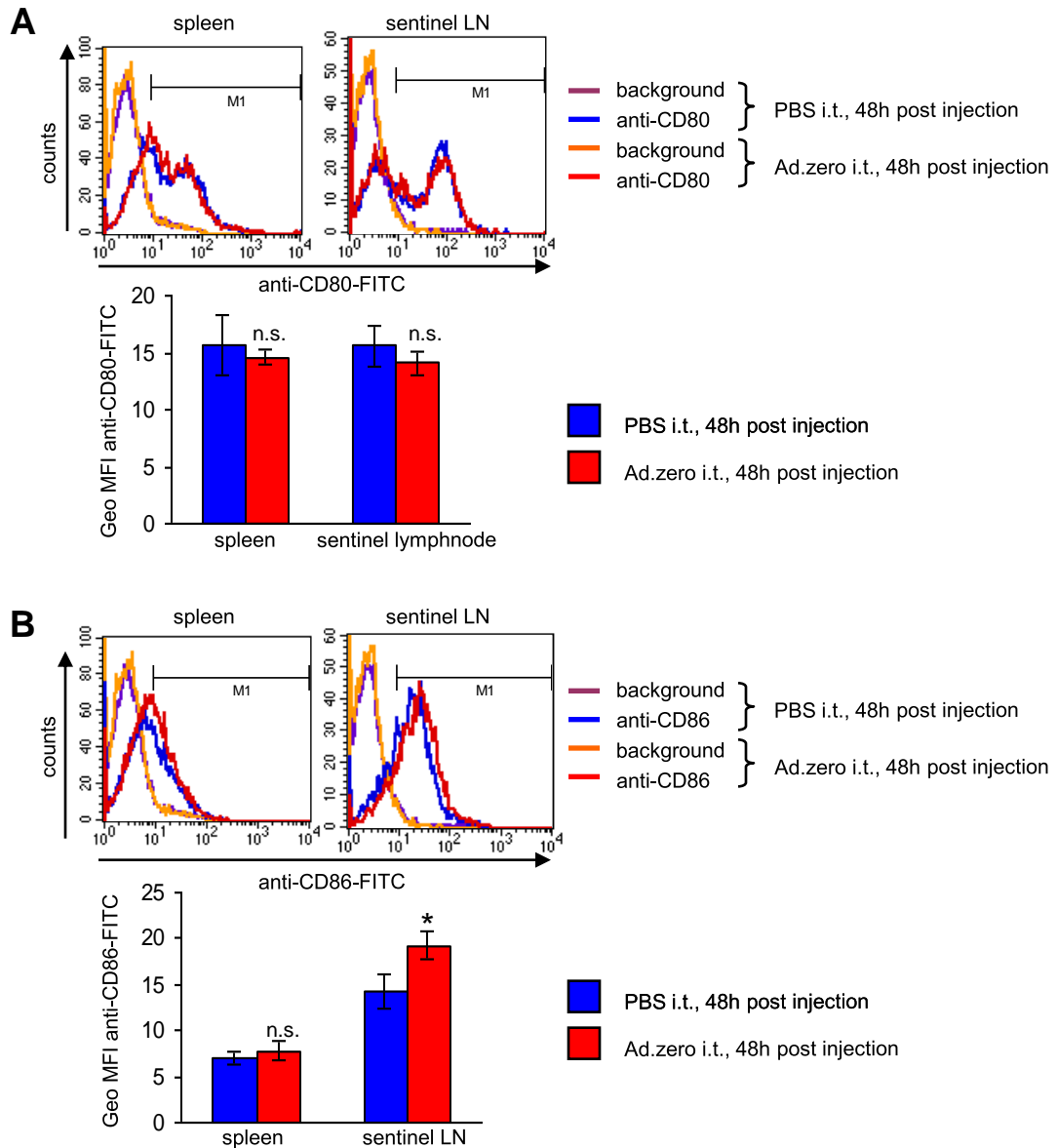
Fig. S13

Fig. S14. CD80 and CD86 surface expression.
1×10^9 Ad.zero (*n*=2 animals) or PBS (*n*=2 animals) was injected into MMC tumors (3-4 mm diameter) in *neu*-transgenic mice. 48 h later spleens and sentinel lymph nodes were harvested, and analyzed with **A**. anti-CD80-FITC or **B.** CD86-FITC via FACS analysis. T cells were excluded from analysis via FSC-SSC pre-gating. *Upper panels.* Overlays of representative flow charts are shown. *Lower panels.* Bars indicate mean and SD. *P*>0.05 *n.s.* (not significant); *, *P*<0.05 (two-sided Student's *t*-test).
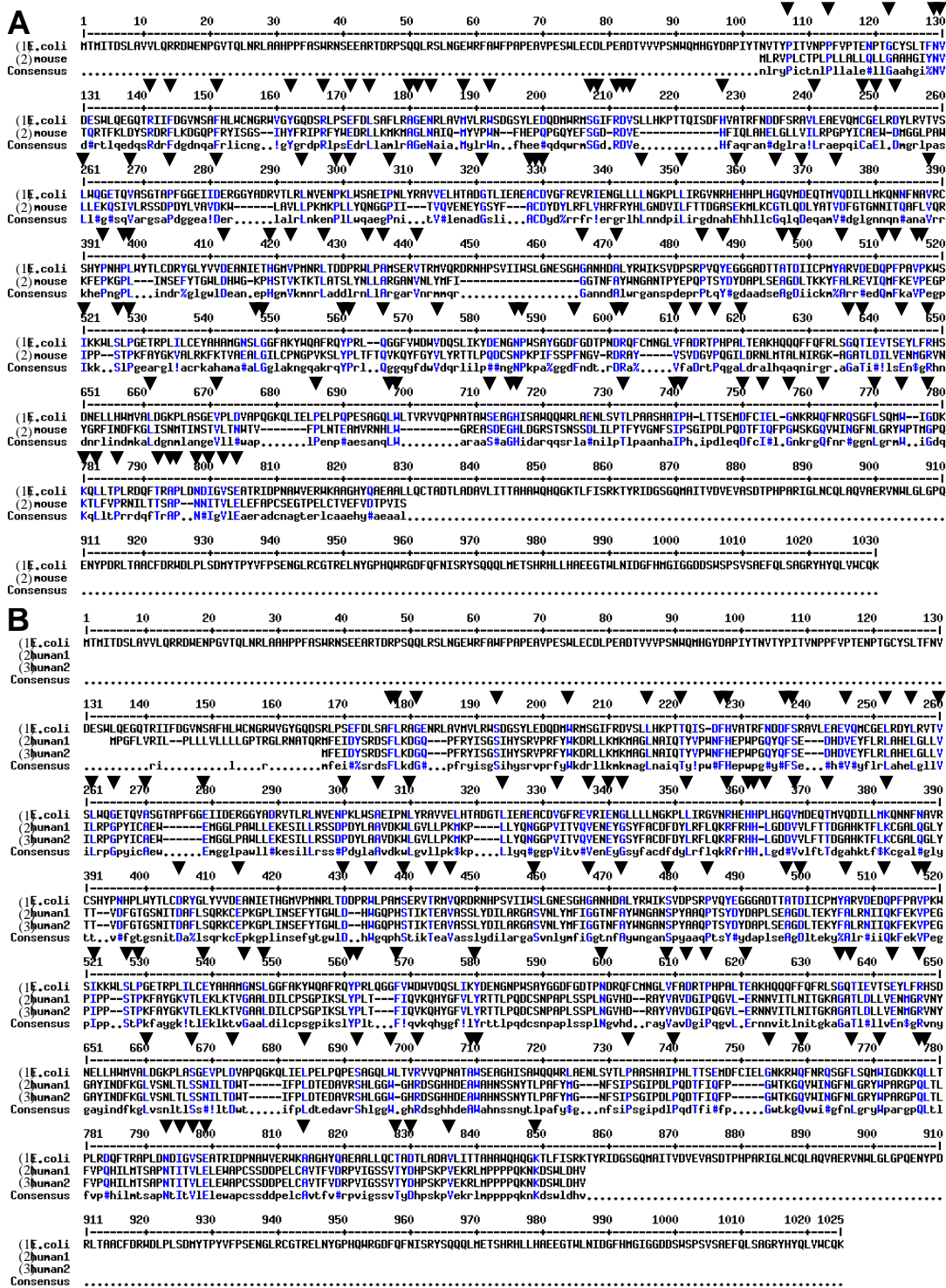
Fig. S14

Fig. S15. Alignment of beta-galactosidase amino acid (aa) sequences.
A. E.coli versus mouse: 11.52% (118aa) homology between E.coli and mouse protein was found (indicated with arrows). *(1)* E.coli beta-D-galactosidase (lacZ; 1024aa, accession#: J01636) and *(2)* mouse beta-1-galactosidase (647aa, accession#: NM_009752). **B. E.coli versus human**: 9.57% (98aa) homology between E.coli and human proteins was found (indicated with arrows). *(1)* E.coli beta-D-galactosidase, *(2)* human beta-1-galactosidase variant1 (677aa, accession#: NM_000404) and *(3)* human beta-1-galactosidase variant2 (647aa, accession#: NM_001079811). Note that the difference between the two human beta-1-galactosidase variants is a N-terminal 30aa sequence that is present in variant1 but not in variant2. Alignments were generated using multi-alignment tool (http://bioinfo.genopole-toulouse.prd.fr/multialin/multialin.html).

Fig. S15

Tab. S1. Primer pairs for real-time PCR.

F, Forward; *R*, Reverse; *bp*, amplicon size. Primers sequences were generated using Primer3 (http://primer3.sourceforge.net/).

accession #			sequence (5' - 3')	bp
NM_007393	mouse b-actin	F	AGAGGGAAATCGTGCGTGAC	
		R	CAATAGTGATGACCTGGCCGT	138
NM_008337	mouse IFN-γ	F	CACGGCACAGTCATTGAAAG	
		R	GCTGATGGCCTGATTGTCTT	197
NM_011577	mouse TGF-β1	F	CCGCAACAACGCCATCTATG	
		R	CTCTGCACGGGACAGCAAT	117
NM_008357	mouse IL-15	F	CGTGCTCTACCTTGCAAACA	
		R	GAAGGTTTTCTCCTCCAGCTC	94
NM_019418	mouse LIGHT	F	GACTGCATCAACGTCTTGGA	
		R	TAAGATGTGCTGCTGGGTTG	117
ref (23)	α-mouse CD3scFv	F	GTCAGGCCAGTCAGGACATT	
		R	AGAACCACTGCCACTGAACC	133
ref (25)	α-mouse CD137scFv	F	ACCAACCTGGAACTGAAACG	
		R	TGCACAGGAGAGTTTCATGG	129
J01636	E.coli lacZ	F	TTGCCGTCTGAATTTGACCT	
		R	CCGCCACATATCCTGATCTT	114
AC_000008	human Ad5 E1A	F	TCTGCCACGGAGGTGTTATT	
		R	TTCCTGCACCGCCAACATTA	214
AC_000008	human Ad5 hexon	F	TACTGCGTACTCGTACAAGG	
		R	AGAGCAGTAGCAGCTTCATC	200
AC_000008	human Ad5 E4	F	TAAGCATAAGACGGACTACG	
		R	GTAAGGCTGACTGTTATGGC	357

Tab. S1

Supplementary Material

Adenovirus vectors:

In this study 12 adenovirus vectors were used. The genomic structures and functions of these vectors are summarized in *Fig. S2*. Vectors are divided into four categories: ***A. Control vector***: Ad.zero was E1/E3-deleted, transgene-devoid and constructed for this study as described below. ***B. Reporter-gene expressing vectors*** were E1/E3-deleted and described previously (1). Ad.GFP (expressing green fluorescent protein under the control of the CMV promotor); Ad.lacZ (expressing E.coli β-galactosidase a.k.a. lacZ under the control of the RSV promotor); Ad.IR-GFP and Ad.IR-lacZ expressing GFP or lacZ in a replication-dependent manner (upon genomic vector replication and homologous recombination between inverted repeats [IR]; see (1) or Fig. S1). ***C. Immunoadjuvant-expressing vectors*** were E1/E3-deleted and constructed for this study. Ad.αCD3 and Ad.αCD137 expressed membrane-bound anti-mouse CD3scFv and anti-mouse CD137scFv under the control of the RSV promotor, respectively ((2, 3) and Fig. S3). Ad.IL-15 and Ad.LIGHT expressed mouse interleukin 15 and mouse LIGHT (TNFSF14) under the control of the RSV promotor, respectively. To produce Ad.αCD3, Ad.αCD137, Ad.IL-15 and Ad.LIGHT the corresponding cDNAs (αCD137 (4); αCD3 (3); IL-15 and LIGHT obtained from InvivoGen, San Diego, CA) were cloned into pAd.RSV under the control of the Rous sarcoma virus (RSV) promoter. For Ad.zero pAd.RSV was transgene-devoid. pAd.RSV was linearized by *Xmn*I digestion and cotransfected with pBHG10 into 293 cells as described before (1). ***D. Oncolytic vectors.*** H101 (generously provided by Dr. Liang Min, Shanghai Sunway Biotech Co., Inc.) was partially deleted in the E1 and E3 regions, which has been shown to restrict vector replication to cancer cells (5-8). We previously developed and characterized E1/E3-deleted

1

Ad.IR-E1A/AP and Ad.IR-E1A/TRAIL vectors that specifically replicate in cancer cells (1). In these vectors the inserted transgenes are expressed strictly upon viral replication upon homologous recombination between inverted repeats (IRs). The inserted transgenes have distinct functions: (i) E1A enhances viral replication, (ii) TRAIL enhances viral spread via induction of apoptosis and (iii) AP as a reporter gene to indicate viral replication ((1, 9) and Fig. S2).

Ad-transduction and Ad-replication assays. For all *in vitro* transduction and replication assays cells were seeded into 24 well plates at a density of $5x10^4$ cells (MMC) or $2.5x10^4$ cells (A549, 293) per well in 1 ml culture medium. 24 h later cells were infected with Ad-vectors (MOI 100 pfu/cell). *(1) Immunoadjuvant expression. Ad.αCD3 and Ad.αCD137*: MMC cells were detached 48 h post transduction using Versene (Gibco). Expression of membrane-bound anti-mouse-CD3/CD137-scFv fusion protein was detected via PE-conjugated goat-anti IgG-Fc antibody (Biosource International, Camarillo, CA). *Ad.IL-15 and Ad.LIGHT*: Supernatants from transduced cells were collected 5 days post infection. Expression of IL-15 and LIGHT proteins was quantified using an IL-15 ELISA Kit (eBioscience, San Diego, CA) and a LIGHT/TNFSF14 ELISA Kit (R&D Systems, Minneapolis, MN) according to the manufacturer's instructions. *(2) Replication-dependent and -independent reporter gene expression.* In these assays MMC cells were transduced with vectors that expressed reporter genes independent (Ad.GFP, Ad-lacZ) or dependent (Ad.IR-GFP, Ad.IR-lacZ, Ad.IR-E1A/AP) on viral genome replication. GFP, lacZ and AP expression was detected as described above. To inhibit adenoviral DNA replication (but not protein synthesis) 3h after transduction, hydroxyurea was added to a subset of wells. *(3) Adenoviral replication assays.* In these assays replication-

2

deficient Ad.zero was compared with replication-competent Ad.IR-E1A/TRAIL. In order to test for viral replication, samples (adherent and floating cells and supernatants) were collected at different time points post infection for quantification of Ad-mRNA, Ad-genomes and Ad plaque-forming-units (pfu). ***Ad-mRNA:*** Before RNA extraction each sample was supplemented with 1 x 10^6 non-infected MMC cells to provide carrier RNA. Viral E1A and hexon transcripts were quantified via real-time PCR. ***Ad-genomes.*** Before DNA extraction each sample was supplemented with 2×10^6 non-infected MMC cells to provide carrier DNA. Viral genomes per ml were subsequently quantified via real-time PCR using primer for the E4 region. ***Ad-pfu.*** Samples were frozen in liquid nitrogen and then thawed at 37°C four consecutive times to release viral particles from cells. Subsequently pfu titering was performed as described above (see *Adenovirus Vectors*). ***Ad-hexon protein.*** Nuclear Ad-hexon protein and surface E-cadherin expression was visualized via immunohistochemistry 3 days post-infection.

Functional evaluation of immunoadjuvant-expressing Ads. For all *in vitro* immunoassays MMC cells were seeded into 24 well plates at a density of 5×10^4 cells per well in 1 ml T cell medium (RPMI-1640 medium containing 10% heat-inactivated FBS, 2mM Gln, 10 mM HEPES, P/S, 50 µM β-mercaptoethanol). 24 h later cells were transduced (MOI 100 pfu/cell) with immunoadjuvant-expressing Ad-vectors. 24 h post transduction splenocytes were added at different target to effector (E:T) ratios. ***Lymphocyte-induced cytotoxicity.*** MMC cells were continuously monitored for CPE and stained with crystal violet when cytotoxicity was observed (see above). ***IFN-γ secretion.*** 48 h post application to MMC cells, non-adherent splenocytes were collected, washed two times with WB and transferred to pre-coated ELIspot plates. 24 h later the spots of IFN-γ-producing cells were determined. ***Lymphocyte proliferation.*** 48 h post

3

MMC-transduction 1 µCi *methyl*-^{3}H thymidine was added per well and incubated for another 16 h. Non-adherent splenocytes were collected from wells and washed three times with 0.5ml ice-cold WB. After the last wash, the supernatant was removed and the cell-associated radioactivity was determined with a scintillation counter.

1. Steinwaerder, D. S., C. A. Carlson, D. L. Otto, Z. Y. Li, S. Ni, and A. Lieber. 2001. Tumor-specific gene expression in hepatic metastases by a replication-activated adenovirus vector. *Nat Med* 7:240-243.
2. Yang, Y., S. Yang, Z. Ye, J. Jaffar, Y. Zhou, E. Cutter, A. Lieber, I. Hellstrom, and K. E. Hellstrom. 2007. Tumor cells expressing anti-CD137 scFv induce a tumor-destructive environment. *Cancer Res* 67:2339-2344.
3. Liao, K. W., Y. C. Lo, and S. R. Roffler. 2000. Activation of lymphocytes by anti-CD3 single-chain antibody dimers expressed on the plasma membrane of tumor cells. *Gene Ther* 7:339-347.
4. Ye, Z., I. Hellstrom, M. Hayden-Ledbetter, A. Dahlin, J. A. Ledbetter, and K. E. Hellstrom. 2002. Gene therapy for cancer using single-chain Fv fragments specific for 4-1BB. *Nat Med* 8:343-348.
5. Nemunaitis, J., I. Ganly, F. Khuri, J. Arseneau, J. Kuhn, T. McCarty, S. Landers, P. Maples, L. Romel, B. Randlev, T. Reid, S. Kaye, and D. Kirn. 2000. Selective replication and oncolysis in p53 mutant tumors with ONYX-015, an E1B-55kD gene-deleted adenovirus, in patients with advanced head and neck cancer: a phase II trial. *Cancer Res* 60:6359-6366.
6. Nemunaitis, J., F. Khuri, I. Ganly, J. Arseneau, M. Posner, E. Vokes, J. Kuhn, T. McCarty, S. Landers, A. Blackburn, L. Romel, B. Randlev, S. Kaye, and D. Kirn. 2001. Phase II trial of intratumoral administration of ONYX-015, a replication-selective adenovirus, in patients with refractory head and neck cancer. *J Clin Oncol* 19:289-298.
7. Khuri, F. R., J. Nemunaitis, I. Ganly, J. Arseneau, I. F. Tannock, L. Romel, M. Gore, J. Ironside, R. H. MacDougall, C. Heise, B. Randlev, A. M. Gillenwater, P. Bruso, S. B. Kaye, W. K. Hong, and D. H. Kirn. 2000. a controlled trial of intratumoral ONYX-015, a selectively-replicating adenovirus, in combination with cisplatin and 5-fluorouracil in patients with recurrent head and neck cancer. *Nat Med* 6:879-885.
8. Yu, W., and H. Fang. 2007. Clinical trials with oncolytic adenovirus in China. *Curr Cancer Drug Targets* 7:141-148.
9. Sova, P., X. W. Ren, S. Ni, K. M. Bernt, J. Mi, N. Kiviat, and A. Lieber. 2004. A tumor-targeted and conditionally replicating oncolytic adenovirus vector expressing TRAIL for treatment of liver metastases. *Mol Ther* 9:496-509.